Research Article

Journal of RAMAN SPECTROSCOPY

Received: 12 April 2009 Accepted: 29 July 2009 Published online in Wiley Interscience: 23 September 2009

(www.interscience.wiley.com) DOI 10.1002/jrs.2471

FT-IR, FT-Raman, SERS spectra and computational calculations of 4-ethyl-*N*-(2′-hydroxy-5′-nitrophenyl)benzamide

C. Yohannan Panicker,[a]* Hema Tresa Varghese,[b] L. Ushakumari,[a] Tugba Ertan,[c] Ilkay Yildiz,[c] Carlos M. Granadeiro,[d] Helena I. S. Nogueira[d] and Y. Shyma Mary[e]

Fourier transform infrared (FT-IR) and FT-Raman spectra of 4-ethyl-*N*-(2′-hydroxy-5′-nitrophenyl)benzamide were recorded and analyzed. A surface-enhanced Raman scattering (SERS) spectrum was recorded in silver colloid. The vibrational wavenumbers and corresponding vibrational assignments were examined theoretically using the Gaussian03 set of quantum chemistry codes. The red shift of the NH stretching wavenumber in the infrared spectrum from the computational wavenumber indicates the weakening of the NH bond resulting in proton transfer to the neighboring oxygen atom. The simultaneous IR and Raman activation of the C=O stretching mode gives the charge transfer interaction through a π-conjugated path. The presence of methyl modes in the SERS spectrum indicates the nearness of the methyl group to the metal surface, which affects the orientation and metal molecule interaction. The first hyperpolarizability and predicted infrared intensities are reported. The calculated first hyperpolarizability is comparable with the reported values of similar derivatives and is an attractive subject for future studies of nonlinear optics. Optimized geometrical parameters of the title compound are in agreement with reported structures.

Supporting information may be found in the online version of this article.

Keywords: benzamide; FT-IR spectra; FT-Raman spectra; DFT calculations; SERS; hyperpolarizability

Introduction

In the past few decades, the dramatically rising prevalence of multidrug-resistant microbial infections has become a serious healthcare problem. In particular, the emergence of multi-drug resistant strains of Gram-positive bacterial pathogens such as methicillin-resistant *Staphylococcus aureus* and *Staphylococcus epidermis* and vancomycin-resistant *Enterococcus* is a problem of ever-increasing significance.[1–5] Benzamide derivatives exhibit various types of biological properties such as anthelmentic, antihistaminic, antifungal, and antibacterial.[6–14] 6-*N*-(2-Hydroxy-3,5-dichlorophenyl)-2-hydroxy-3,5,6-trichlorobenzamide (oxyclozanide), which has a benzamide structure, was discovered in 1969 as an anthelmentic agent effective against *Fasciola hepatica* for the treatment of liver fluke infection.[6] 3,4-Dihydroxy-6-(*N*-ethylamino)benzamide is a natural product that has been found in green pepper (*Piper nigrum L.*) as an antibacterial by Pradhan *et al*.[11] Additionally, a benzamide derivative, BAS-118, has been found to be a novel anti-*Helicobacter pylori* agent with a potent and selective antibacterial activity, which includes clarithromycin (CAM)- and metronidazole (MNDZ)-resistant isolates.[15] Yalcin *et al*.[10,12–14] reported some novel microbiologically active *N*-(2–hydroxy-5-substitutedphenyl) benzamide/phenyl acetamide/phenoxy acetamide/thiophenoxy acetamide derivatives. The synthesis and biological evaluation of *N*-(2-hydroxy-4(or5)-nitro/aminophenyl) benzamides and phenyl acetamides as antimicrobial agents have been reported by Ertan *et al*.[16] 2-Hydroxy-*N*-phenylbenzamides have been reported as a class of compounds with a wide variety of interesting biological activities, including antimycobacterial and antifungal effects.[17–21] Arslan *et al*.[22] reported the molecular structure and vibrational spectra of 2-chloro-*N*-(diethyl carbamothioyl) benzamide by Hartree–Fock (HF) and density functional methods. Takeuchi *et al*.[23] reported the molecular structure of benzamide as studied by gas-phase electron diffraction. Gas-phase structures of fundamental amides, formamide,[24] and acetamide[25] were determined by electron diffraction, and their crystal structures were studied by X-ray and neutron diffraction.[26–30] The crystal structures of benzamide were determined by X-ray and neutron diffraction.[31,32] The hydrogen-bonding interactions between

* *Correspondence to: C. Yohannan Panicker, Department of Physics, TKM College of Arts and Science, Kollam 691 005, Kerala, India. E-mail: cyphyp@rediffmail.com*

a *Department of Physics, TKM College of Arts and Science, Kollam 691 005, Kerala, India*

b *Department of Physics, Fatima Mata National College, Kollam 691 001, Kerala, India*

c *Faculty of Pharmacy, Department of Pharmaceutical Chemistry, Ankara University, Tandogan 06100, Ankara, Turkey*

d *Department of Chemistry, CICECO, University of Aveiro, 3810-193 Aveiro, Portugal*

e *Thushara, Neethinagar-64, Pattathanam, Kollam 691 021, Kerala, India*

thioacetamide and several *N*,*N*-disubstituted benzamides have been studied using near-infrared absorption spectroscopy.[33] Kawski *et al*.[34] reported the X-ray and IR investigation as well as quantum mechanical calculations of 2-hydroxy-benzamides. To our knowledge, no theoretical HF or density functional theory (DFT) calculations, or detailed vibrational infrared and Raman analyses, have been performed on the title compound. A detailed quantum chemical study will aid in understanding the vibrational modes of the title compound and clarifying the experimental data available for this molecule. DFT calculations are known to provide excellent vibrational wavenumbers of organic compounds if the calculated wavenumbers are scaled to compensate for the approximate treatment of electron correlation, for basis set deficiencies, and for the anharmonicity effects.[35–40] DFT is now accepted as a popular post-HF approach for the computation of molecular structure, vibrational wavenumbers, and energies of molecules by the *ab initio* community.[41] In this work, by using HF, B3PW91 and B3LYP methods, we calculated the vibrational wavenumbers of the title compound in the ground state to distinguish the fundamentals from the many experimental vibrational wavenumbers and geometric parameters. These calculations are valuable for providing insight into the vibrational spectrum and molecular parameters. The surface-enhanced Raman scattering(SERS) spectrum is also recorded and analyzed.

Experimental

The chemicals were purchased from commercial vendors and used without purification. The reactions were monitored and the purity of the product was checked by thin-layer chromatography (TLC). Silica gel 60 F_{254} chromatoplates were used for TLC. The solvent systems were chloroform/methanol (15 : 1). The final compound was purified by recrystallization in ethanol. The melting point was measured with a capillary melting point apparatus (Buchi SMP 20 and Electrothermal 9100) and is uncorrected. The yield was calculated after recrystallization. The Fourier transform infrared (FT-IR) spectrum (Fig. 1) was recorded on a Jasco FT/IR-420 spectrometer with KBr pellets. The FT-Raman spectra (Figs. 2 and 3) were obtained on a Bruker RFS 100/S, Germany. For excitation of the spectrum, the emission from a Nd : YAG laser was used (excitation wavelength 1064 nm, maximum power 150 mW). The measurements were made on solid sample. The aqueous silver colloid used in the SERS experiments was prepared by reduction of silver nitrate by sodium citrate, using the Lee – Meiser method.[42] Solutions of the title compound were made up in ethanol (0.1 mmol in 1 ml of solvent) and transferred by a microsyringe into the silver colloid (10 µl in 1 ml of colloid) such that the overall concentration was 10^{-3} mol dm^{-3}. Colloid aggregation was induced by addition of an aqueous solution of $MgCl_2$ (1 drop of a 2 mol dm^{-3} solution). Polyvinylpyrrolidone was then used to stabilize the colloid (1 drop of 0.1 g 10 ml^{-1} aqueous solution). The final colloid mixture was placed in a glass tube and the Raman spectrum registered.

The ^{1}H NMR spectra was recorded by employing a VARIAN Mercury 400 MHz FT spectrometer; the chemical shifts (δ) are in parts per million relative to TMS, and coupling constants (J) are reported in Hertz. Elemental analyses were carried out on a Leco 932 CHNS-O analyzer. The results of the elemental analyses (C, H, N) were within ±0.4% of the calculated amounts.

The synthesis was performed by reacting 2-amino-4-nitrophenol with *p*-ethylbenzoic acid chloride, which was obtained in turn by treating *p*-ethylbenzoic acid with thionyl chloride. Thionyl chloride (1.5 ml) and *p*-ethylbenzoic acid (0.5 mmol) were refluxed in benzene (5 ml) at 80 °C for 3 h, and then excess thionyl chloride was removed *in vacuo*. The residue was dissolved in ether (10 ml), and the solution was added during 1 h to a stirred, ice cold mixture of 2-amino-4-nitrophenol (0.5 mmol), sodium bicarbonate (0.5 mmol), diethyl ether (10 ml), and water (10 ml). The mixture

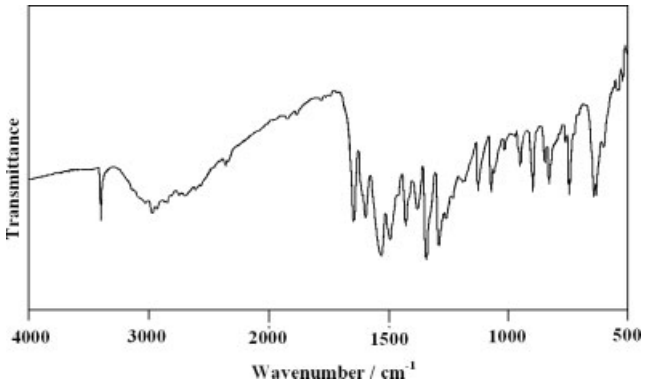

Figure 1. FT-IR spectrum of 4-ethyl-*N*-(2′-hydroxy-5′-nitrophenyl) benzamide.

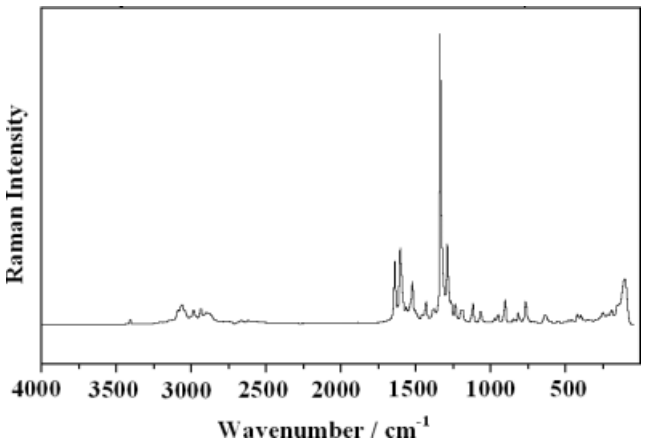

Figure 2. FT-Raman spectrum of 4-ethyl-*N*-(2′-hydroxy-5′-nitrophenyl) benzamide.

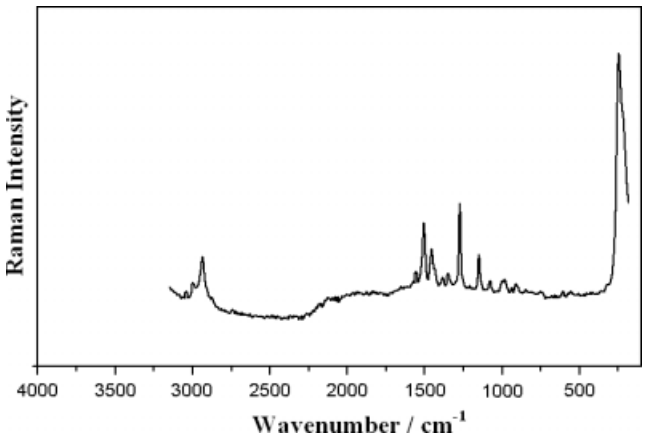

Figure 3. SERS spectrum of 4-ethyl-*N*-(2′-hydroxy-5′-nitrophenyl) benzamide.

Journal of RAMAN SPECTROSCOPY

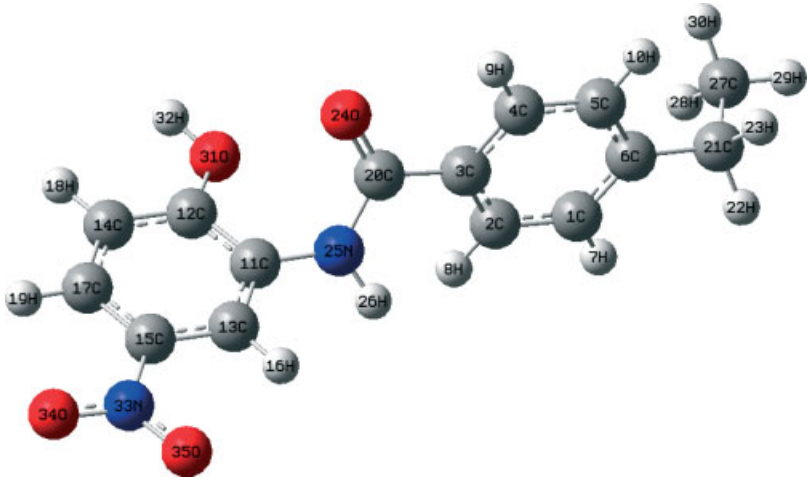

Figure 4. Optimized geometry of 4-ethyl-*N*-(2′-hydroxy-5′-nitrophenyl)benzamide.

was stirred overnight at room temperature and filtered. The precipitate was washed with water, 2N HCl, water, respectively and finally with ether to give the compound. The crude product was purified by recrystallization from ethanol. The crystal was dried *in vacuo*.

M.p. 254–256 °C; Yield 46%; Elemental analyses: calculated: C62.93, H 4.93; N 9.79; found: C 62.58; H 5.218; N 9.788. ^{1}H NMR (DMSO-d_6) δ ppm J (in Hz): 1.21 (t, 3H, CH_3), 2.69(q, 2H, CH_2), 7.08(d, 1H, $J_0 = 9.2$, 3′-H); 7.38(d, 2H, $J_0 = 8.4$, 3-H, 5-H); 7.91(d, 2H, $J_0 = 8.8$, 2-H, 6-H); 7.99(dd, 1H, $J_0 = 9.2$ and $J_m = 2.8$, 4′-H); 8.78(d, 1H, $J_m = 3.2$, 6′-H); 9.55(s, 1H, OH).

Computational Details

The vibrational wavenumbers were calculated using the Gaussian03 software package on a personal computer.[43] The computations were performed at HF/6-31G*, B3PW91/6-31G*, and B3LYP/6-31G* levels of theory to get the optimized geometry (Fig. 4) and vibrational wavenumbers of the normal modes of the title compound. Parameters corresponding to optimized geometry of the title compound are given in table S1 (Supporting Information). The DFT partitions, the electronic energy $E = E_T + E_V + E_J + E_{XC}$, where E_T, E_V, and E_J are electronic kinetic energy, electron nuclear attraction, and electron–electron repulsion terms, respectively. The electron correlation is taken into account in the DFT via the exchange-correlation term E_{XC}, which includes exchange energy arising from the antisymmetry of the quantum mechanical wave function and dynamic correlation in the motion of individual electron, and it makes the DFT calculations dominant over conventional HF procedure.[44] DFT calculations were carried out with Becke's three-parameter hybrid model using the Lee–Yang–Parr correlation functional (B3LYP) method. Molecular geometries were fully optimized by Berny's optimization algorithm using redundant internal coordinates. Harmonic vibrational wavenumbers were calculated using analytic second derivatives to confirm the convergence to minima in the potential surface. At the optimized structure of the examined species, no imaginary wavenumber modes were obtained, proving that a true minimum on the potential surface was found. The optimum geometry was determined by minimizing the energy with respect to all geometrical parameters without imposing molecular symmetry constraints. The DFT hybrid B3LYP functional tends also to overestimate the fundamental modes; therefore, scaling factors have to be used for obtaining a considerably better agreement with experimental data.[45] Scaling factors 0.9613 and 0.8929 have been uniformly applied for the DFT- and HF-calculated wavenumbers.[44] The observed disagreement between theory and experiment could be a consequence of the anharmonicity and of the general tendency of the quantum chemical methods to overestimate the force constants at the exact equilibrium geometry.[40] The assignments of the calculated wavenumbers is aided by the animation option of the MOLEKEL program, which gives a visual presentation of the vibrational modes.[46,47]

Results and Discussion

The observed IR and Raman bands with their relative intensities and calculated (scaled) wavenumbers and assignments are given in Table 1.

IR and Raman spectra

The OH group provides three normal vibrations: the stretching vibration υOH, and the in-plane and out-of-plane deformations δOH and γOH. The B3LYP calculations give the υOH band at 3604 cm^{-1}. The in-plane OH deformation[48] is expected in the region 1400 ± 40 cm^{-1}, and the band at 1410 cm^{-1} in the Raman spectrum and 1405 cm^{-1} by DFT is assigned as this mode, which is not pure but contains significant contribution from phenyl ring-stretching modes. The stretching of the hydroxyl group with respect to the phenyl moiety $\upsilon(C-O)_h$ appears at 1272 cm^{-1} in the Raman spectrum, and the calculated value is 1268 cm^{-1}. This band is expected in the[49–51] region 1220 ± 40 cm^{-1}. The out-of-plane OH deformation is expected[48] generally in the region 650 ± 80 cm^{-1}, and in our case it is at 632 cm^{-1} in the IR spectrum and at 628 cm^{-1} theoretically. For paracetamol, $\upsilon(C-O)_h$ and γOH are reported at 1240 and 620 cm^{-1}, respectively.[52]

The vibrations of the CH_2 group (the asymmetric stretch $\upsilon_{as}CH_2$, symmetric stretch υ_sCH_2, the scissoring vibrations δCH_2, and the wagging vibration ωCH_2) appear in the regions 2940 ± 20, 2885 ± 45, 1440 ± 10, and 1340 ± 25 cm^{-1}, respectively.[48,50] These bands are observed at 2971, 1431 cm^{-1} in the IR spectrum, 2976, 2920, 1457 cm^{-1} in the Raman spectrum, and at 2963, 2929, 1459, 1319 cm^{-1} theoretically for the title compound. According to literature,[53] the scissoring mode of the CH_2 group gives rise to

Table 1. Calculated vibrational wavenumbers (scaled) as well as measured infrared and Raman band positions and assignments for 4-ethyl-*N*-(2′-hydroxy-5′-nitrophenyl)benzamide

HF/6-31G*		B3PW91/6-31G*		B3LYP/6-31G*					
υ (cm^{-1})	IR intensity	υ (cm^{-1})	IR intensity	υ (cm^{-1})	IR intensity	$\upsilon_{(IR)}$ (cm^{-1})	$\upsilon_{(Raman)}$ (cm^{-1})	$\upsilon_{(Raman)}$ (cm^{-1})	Assignments
3671	131.17	3640	88.02	3604	76.45				υOH
3477	40.94	3491	19.88	3470	16.62	3408 sbr	3402 w		υNH
3071	1.50	3137	2.87	3131	2.37	3124 w	3136 w		υCH I
3066	2.73	3122	3.61	3117	3.23				υCH I
3043	2.63	3107	2.53	3100	2.63				υCH II
3016	18.54	3082	13.19	3073	14.66		3079 w		υCH II
3006	12.32	3071	10.98	3061	12.39				υCH I
3000	20.78	3068	17.01	3059	19.51		3055 m	3050 w	υCH II
2996	17.70	3064	14.77	3055	16.09	3042 w	3039 w	3040 w	υCH II
2927	49.95	3021	27.65	3004	31.73				υ_{as}Me
2920	65.66	3018	41.70	3001	46.63	2999 w			υ_{as}Me
2897	6.55	2980	7.92	2963	8.87	2971 m	2976 w		$\upsilon_{as}CH_2$
2870	33.02	2941	34.35	2933	35.53			2933 s	υ_{s}Me
2861	43.58	2940	29.48	2929	30.42		2920 w		$\upsilon_{s}CH_2$
						2887 br	2883 w		Overtones/combinations
						2832 w	2661 w		
						2759 w			
						2704 w			
						2558 w			
						2102 w			
						2029 w			
						1883 w			
						1810 w			
1752	297.17	1730	173.50	1712	170.70	1647 s	1630 s		υC═O
1661	394.26	1630	92.65	1609	43.98				υPh I
1626	44.34	1616	31.75	1604	26.86	1598 s			υPh II
1607	125.64	1603	63.43	1589	54.87		1587 s		υPh I
1596	69.44	1589	140.84	1560	13.78				υPh II
1576	9.96	1572	5.30	1559	184.82	1530 vs	1550 w	1533 w	$\upsilon_{as}NO_2$
1518	167.28	1508	92.82	1501	10.89		1508 m	1504 s	υPh II
1513	49.95	1502	58.43	1497	79.83	1497 vs	1494 sh		υPh I
1495	286.85	1478	312.36	1479	12.19				δ_{as}Me
1477	3.81	1473	10.79	1472	322.37				δNH
1465	6.79	1463	9.54	1468	7.78	1468 w			δ_{as}Me
1461	0.23	1454	2.13	1459	1.41	1431 m	1457 w	1452 m	υPh I, δCH_2
1457	407.85	1411	116.50	1405	79.35		1410 m	1430 w	υPh II, δOH
1410	273.34	1401	25.56	1397	90.69				δOH
1402	51.42	1376	2.28	1381	1.84	1383 m	1377 w	1378 w	δ_{s}Me
1394	1.06	1366	328.42	1346	12.33				υCN
1336	9.69	1363	259.58	1339	433.60	1345 vs		1340 w	$\upsilon_{s}NO_2$
1311	26.10	1333	0.58	1319	8.58				ωCH_2
1304	334.21	1315	6.13	1316	0.16				υPh II
1277	9.46	1303	225.71	1297	120.52		1304 vvs		υCN
1254	90.64	1291	7.86	1290	262.08	1292 s			υPh I
1249	179.69	1275	270.91	1268	216.74		1272 s	1272 s	$\upsilon(C\text{-}O)_h$
1235	7.65	1237	1.39	1237	0.63	1240 w	1244 w		τCH_2
1205	3.68	1235	2.52	1233	28.90				υPh I
1180	5.36	1225	130.25	1218	140.90	1220 s	1217 w		δNH
1178	2.46	1194	2.79	1188	7.73	1185 w	1180 w	1184 w	δCH II
1168	27.06	1168	35.84	1170	43.77			1149 s	ρMe
1122	16.69	1154	29.37	1153	22.45				ρNH
1113	6.20	1111	14.01	1109	14.81	1127 m			δCH II

Table 1. (*Continued*)

HF/6-31G*		B3PW91/6-31G*		B3LYP/6-31G*					
υ (cm^{-1})	IR intensity	υ (cm^{-1})	IR intensity	υ (cm^{-1})	IR intensity	$\upsilon_{(IR)}$ (cm^{-1})	$\upsilon_{(Raman)}$ (cm^{-1})	$\upsilon_{(Raman)}$ (cm^{-1})	Assignments
1091	73.06	1107	5.6971	1109	13.91		1106 m		δCH II
1074	2.43	1086	52.97	1079	56.61	1072 m		1072 w	δCH I
1069	104.88	1067	108.57	1063	103.51	1066 sh	1069 m		δCH I
1057	8.97	1051	22.62	1049	20.75				ρMe
1032	6.35	1037	5.51	1038	6.88				δCH I
998	2.41	998	9.79	999	11.75	1015 w			δCH II
995	4.31	952	3.44	952	1.15	949 w	960 w	975 w	γCH II
981	0.27	950	1.85	941	2.29		939 w		υC21C27
976	0.19	935	22.48	931	12.09				γCH II
960	9.83	928	11.48	925	21.36				γCH II
933	25.40	920	2.41	920	2.90			914 w	γCH I
929	2.08	903	10.65	902	9.13	897 m	902 m	906 w	γCH I
886	26.23	871	21.63	869	19.13				ωNH
862	15.16	836	17.31	837	14.67	847 m	846 w		γCH II
850	10.29	823	12.34	823	10.74	827 m		829 w	Ring breath II
828	23.61	806	6.45	800	7.39		809 w		δNO_2
824	6.22	795	14.92	794	14.88				γCH II
779	17.59	780	5.83	776	5.17				RING I
769	21.44	767	1.66	769	0.84		772 m		ρCH_2
767	59.08	764	1.28	761	1.65	759 w			δPh II, γNH
763	0.96	747	18.70	746	16.90	743 m			δC═O
757	11.64	732	34.24	724	29.16	727 w	717 w	730 w	ωNO_2
709	8.90	695	15.60	693	15.40	698 w			γPh II
698	11.78	682	12.28	680	11.80				γPh I
639	39.16	639	19.52	636	19.81	641 m	643 w		δPh(X) II
625	0.58	624	0.31	628	0.30	632 m			δPh(X) I, γOH
617	5.69	620	2.25	621	2.88	618 w	616 w	601 w	δPh II
580	37.58	577	27.25	577	25.46				γPh(X) I
553	2.06	553	2.26	553	1.85	545 w	550 w		γPh II
535	1.53	534	1.73	534	1.14	524 w		534 w	ρNO_2
510	6.70	506	8.57	508	8.27	505 w			γPh II (X)
470	14.54	475	54.45	475	50.80		476 w		NH
463	1.89	464	17.48	464	13.40				δPh (X) I
418	1.19	451	32.90	450	37.96				δCN(X) I
409	0.13	407	13.42	408	13.07		412 w		δPh (X)II
375	30.14	399	0.19	402	0.34		402 w		γPhII
355	5.82	360	2.30	362	3.01				δCC(X) II
344	35.58	353	50.30	352	10.99				γPh(X) I
339	42.23	350	19.10	347	49.39		346 w		δCO(X) I
329	2.13	332	14.72	332	18.18				Ch2
302	67.78	320	15.22	320	19.92				τMe
296	40.66	296	3.47	297	3.54				γCC(X) II
269	9.93	268	6.10	270	6.43		266 w		τMe
234	13.27	235	4.37	236	4.24			244 vs	γCO(X) I
214	0.22	215	0.09	212	0.10		217 w		γCO(X) I
192	1.37	190	0.93	191	1.02				γCN(X) I
173	6.22	174	2.54	175	2.36		180 w		δCN(X) I
125	4.23	136	3.52	138	3.51				γCN(X) I
121	0.85	122	2.19	123	2.08				γCN(X) I
81	2.31	89	5.71	90	5.87		101 m		γCC(X) II

υ, stretching; δ, in-plane bending; γ, out-of-plane bending; τ, torsion; s, strong; m, medium; w, weak; v; very; br, broad; Ph I and Ph II, tri- and *para*-substituted phenyl rings; X, substituent sensitive; subscript: as, asymmetric, s, symmetric.

a characteristic band near 1465 cm^{-1} in the IR and Raman spectra. This mode is unambiguously correlated with the strong band at 1457 cm^{-1} in the Raman spectrum. The twisting and rocking vibrations of the CH_2 group appear in the regions[48] 1260 ± 10 and 800 ± 25 cm^{-1}. These modes are also assigned (Table 1).

For the methyl group, the asymmetric stretching vibration is observed in the region 2940–3010 cm^{-1}, and the symmetric stretching appear in the region[48] 2840–2970 cm^{-1}. The computed wavenumbers of the modes corresponding to the $\upsilon_{as}CH_3$ and υ_sCH_3 group are 3004, 3001, and 2933 cm^{-1}. The asymmetric deformations[48] of the methyl group are expected in the regions 1465 ± 20 and 1445 ± 25 cm^{-1}. The overlap between the two regions is quite considerable, so for many molecules the deformations often coincide. The symmetric deformation[48] of methyl group appears in the region 1380 ± 20 cm^{-1}. The B3LYP calculations give bands at 1479, 1468 and 1381 cm^{-1} as asymmetric and symmetric deformations of the methyl group, respectively. Also, the theoretically calculated values for rocking modes of the methyl group are 1049 and 1170 cm^{-1}, which are expected in the regions[48] 1080 ± 80 and 1170 ± 95 cm^{-1}. The torsional modes of methyl group are observed below 400 cm^{-1}.

The carbonyl stretching C═O vibrations[48,54] are expected in the region 1715–1680 cm^{-1} and in the present study this mode appears at 1647 cm^{-1} in the IR spectrum and at 1630 cm^{-1} in the Raman spectrum as a strong band. The B3LYP calculations give this mode at 1712 cm^{-1}. El-Shahawy *et al.*[52] reported a value 1640 cm^{-1} in the IR spectrum as υC═O for paracetamol. The deviation of the calculated wavenumber for this mode can be attributed to the underestimation of the large degree of π-electron delocalization due to conjugation in the molecule.[55] The intensity of the carbonyl group can increase because of conjugation or formation of hydrogen bonds. The increase in conjugation, therefore, leads to the intensification of the Raman lines as well as increased IR band intensities. The conjugation and influence of intermolecular hydrogen bonding result in the lowering of the stretching wavenumber. The bands associated with the C═O stretching mode are found to be strongly and simultaneously active in both IR and Raman spectra.

The NH stretching vibration[48] appears as a strong and broad band in the region 3390 ± 60 cm^{-1}. For the title compound, the strong band at 3408 cm^{-1} in the IR spectrum and 3402 cm^{-1} in the Raman spectrum is assigned as the υNH mode. The calculated value for this mode is 3470 cm^{-1}. The NH stretching wavenumber, which is very strong in the IR spectrum, is red-shifted by 62 cm^{-1} from the computed wavenumber (B3LYP). This indicates the weakening of the NH bond resulting in proton transfer to the neighboring oxygen.[54] The CNH vibration, in which the N and H atoms move in opposite direction of the carbon atoms in the amide moiety, appears at 1472 cm^{-1} theoretically, and, the CNH vibration, in which the N and H atoms move in the same direction of the carbon atoms in the amide group, appears at 1220 (IR), 1217 (Raman), and 1218 cm^{-1} (DFT).[49,50,52] The calculated value of the NH rocking[52] is 1153 cm^{-1}. The out-of-plane wagging[48] of NH is moderately active with a broad band in the region 790 ± 70 cm^{-1}, and the band at 869 cm^{-1} (DFT) is assigned as this mode. El-shahawy *et al.*[52] reported this band at 720 cm^{-1}.

The C–N stretching vibration[48] coupled with δNH is moderately to strongly active in the region 1275 ± 55 cm^{-1}. El-Shahawy *et al.*[52] observed a band at 1320 cm^{-1} as this υC–N mode. In the present case, the band at 1304 cm^{-1} in the Raman spectrum is assigned to this mode. The DFT calculations give the corresponding band at 1297 cm^{-1}.

The most characteristic band in the spectra of the nitro compounds are due to NO_2 stretching vibrations, which are the two most useful group wavenumbers, not only because of their spectral position but also for their strong intensity.[48] In nitro compounds, the antisymmetric NO_2 stretching modes[48] are located in the region 1580 ± 80 cm^{-1}. The symmetric NO_2 stretching vibrations[48] are expected in the region 1380 ± 20 cm^{-1}. In substituted nitrobenzenes, υ_sNO_2 appears strongly at 1345 ± 30 cm^{-1}; in 3-nitropyridine[56] at 1350 ± 20 cm^{-1}; and in conjugated nitroalkenes[57] at 1345 ± 15 cm^{-1}. In the present case, the bands observed at 1530 cm^{-1} in the IR spectrum and 1550 cm^{-1} in the Raman spectrum are assigned as asymmetric NO_2 stretching modes. The symmetric NO_2 stretching mode is observed at 1345 cm^{-1} as a very strong band. The DFT calculations give 1559 and 1339 cm^{-1} as asymmetric and symmetric stretching NO_2 vibrations. According to some investigators,[58–60] the NO_2 scissoring[48] occur in the region 850 ± 60 cm^{-1} when conjugated to C═C or aromatic molecules, with a contribution of the υCN, which is expected to be near 1120 cm^{-1}. For nitrobenzene, δNO_2 is reported[48] at 852 cm^{-1}; for $H_2C{=}CHNO_2$ at 890 cm^{-1}; and for 1,3-dinitrobenzene at 904 and 834 cm^{-1}. For the title compound, the DFT calculations give the band at 800 cm^{-1} as the deformation band of NO_2. The band observed at 809 cm^{-1} in the Raman spectrum is assigned as δNO_2. In aromatic compounds, the wagging mode ωNO_2 is assigned at 740 ± 50 cm^{-1} with moderate to strong intensity, a region in which γCH is also active.[48] ωNO_2 is reported at 701 and 728 cm^{-1} for 1,2-dinitrobenzene and at 710 and 772 cm^{-1} for 1,4-dinitrobenzene[48]. For the title compound, the band at 727 cm^{-1} in the IR spectrum, 717 cm^{-1} in the Raman spectrum, and 724 cm^{-1} by DFT are assigned as the wagging modes of NO_2. In aromatic compounds, the rocking mode ρNO_2 is active in the region 545 ± 45 cm^{-1}. Nitrobenzene[48] shows this rocking mode at 531 cm^{-1}. In the present case, the DFT calculations give ρNO_2 at 534 cm^{-1}. Sundaraganesan *et al.*[61] reported the NO_2 deformation bands at 839, 744, and 398 cm^{-1} (experimental) and 812, 716, 703, and 327 cm^{-1} theoretically. The identification of C–N stretching vibration is a difficult task because mixing of several bands is possible in this region. Silverstein *et al.*[53] assigned the C–N stretching absorption in the region 1382–1286 cm^{-1} for aromatic amines. The C–N stretching mode is reported at 1368 cm^{-1} for benzamide,[62] at 1382, 1307 cm^{-1} for benzotriazole[61] and at 1335 and 1331 cm^{-1} for 2,4-dinitrophenylhydrazine.[61] Primary aromatic amines with nitrogen directly on the ring absorbs strongly at 1330–1260 cm^{-1} due to stretching of the phenyl carbon–nitrogen bond.[50] The reported values of the C–N stretching modes are 1340 cm^{-1} (Raman), 1325 (calculated),[63] 1318 cm^{-1}[64] and at 1332 (IR), 1315 (Raman), 1315 cm^{-1} (HF).[65] For the title compound, the B3LYP calculations give the stretching mode of CN at 1346 cm^{-1}.

Since the identification of all the normal modes of vibration of large molecules is not trivial, we tried to simplify the problem by considering each molecule as a substituted benzene. Such an idea has already been successfully utilized by several workers for the vibrational assignment of molecules containing multiple homo and hetero aromatic rings.[65–70] In the following discussion, the tri-substituted and *para*-substituted phenyl rings are designated as ring I and II, respectively. The modes in the two phenyl rings will differ in wavenumber, and the magnitude of splitting will depend on the strength of interaction between different parts (internal coordinates) of the two rings. For some modes, this splitting is so small that they may be considered as quasi-degenerate,

and for other modes a significant amount of splitting may be observed.[66–68,71]

The aromatic CH stretching vibrations[48] absorb weakly to moderately between 3120 and 3000 cm^{-1}. The B3LYP calculations give bands in the range 3055–3131 cm^{-1} as υCH stretching modes. Experimentally, we have observed bands at 3124 and 3042 cm^{-1} in the IR spectrum and at 3136, 3079, 3055, and 3039 cm^{-1} in the Raman spectrum as CH stretching modes of the phenyl rings.

The benzene ring possess six ring-stretching vibrations of which the four with the highest wavenumbers occurring near 1600, 1580, 1490 and 1440 cm^{-1} are good group vibrations.[48] With heavy substituents, the bands tend to shift to somewhat lower wavenumbers, and the greater the number of substituents on the ring, the broader the absorption regions.[48] In the case of C═O substitution, the band near 1490 cm^{-1} can be very weak.[48] The fifth ring-stretching vibration is active near 1315 ± 65 cm^{-1}, a region that overlaps strongly with that of the CH in-plane deformation.[48] The sixth ring-stretching vibration, the ring-breathing mode, appears as a weak band near 1000 cm^{-1} in mono-, 1,3-di-, and 1,3,5-trisubstituted benzenes. In the otherwise substituted benzenes, however, this vibration is substituent-sensitive and difficult to distinguish from other modes. The ring-breathing mode for the *para*-substituted benzenes with entirely different substituents[49] has been reported to be strongly IR active with typical bands in the interval 780–840 cm^{-1}. For the title compound, this is confirmed by the band in the IR spectrum at 827 cm^{-1}, which finds support from the computational results. The ring-breathing mode of *para*-substituted benzenes are reported at 804 and 792 cm^{-1} experimentally and at 782 and 795 cm^{-1} theoretically.[72,73] In asymmetric tri-substitued benzenes, when all the three substituents are light, the wavenumber interval of the breathing mode[49] is between 500 and 600 cm^{-1}. When all the three substituents are heavy, the wavenumber appears above 1100 cm^{-1}. In the case of mixed substituents, the wavenumber is expected[49] to appear between 600 and 750 cm^{-1}. For the title compound, the phenyl ring I breathing mode is observed at 776 cm^{-1} theoretically. For *para*-substituted benzenes, the δCH modes are seen in the range 995–1315 cm^{-1} and for tri-substituted benzenes these modes are in the range[48] 1290–1050 cm^{-1}. Bands observed at 1185, 1127, 1072, 1066, and 1015 cm^{-1} in the IR spectrum and at 1180, 1106, and 1069 cm^{-1} in the Raman spectrum are assigned as δCH modes. The DFT calculation give these modes at 1188, 1109, 1079, 1063, 1038, and 999 cm^{-1}, as these modes and some of the bands are not pure but contain significant contribution from other modes. The CH out-of-plane deformations[48] are observed between 1000 and 700 cm^{-1}. Generally, the CH out-of-plane deformations with the highest wavenumbers are weaker than those absorbing at lower wavenumbers. These γCH modes are observed at 949, 897, and 847 cm^{-1} in the IR spectrum and at 960, 902, and 846 cm^{-1} in the Raman spectrum. The strong CH out-of-plane deformation band occurring at 840 ± 50 cm^{-1} is typical for 1,4-di-substituted benzenes.[48] For the title compound, a band is observed at 847 cm^{-1} in the IR spectrum. Again according to literature,[48,50] a lower γCH absorbs in the neighborhood 820 ± 45 cm^{-1}, but is much weaker or infrared inactive. The DFT calculation gives a γCH at 794 cm^{-1} and no band is experimentally observed for this mode. In the case of tri-substituted benzenes, two γCH bands are observed at 890 ± 50 and 815 ± 45 cm^{-1} in the IR spectrum. The bands observed at 897 (IR), 902 (Raman), and 902 cm^{-1} (DFT) are assigned to this modes.

The IR bands in the 2887–1810 cm^{-1} region and their large broadening support the intramolecular hydrogen bonding between the C═O and OH groups.[74]

SERS spectrum

The relative intensities in the SERS spectrum are expected to differ significantly from normal the Raman spectrum due to specific selection rules.[75] Surface selection rules suggest that for a molecule adsorbed flat on the silver surface, its out-of-plane bending modes will be more enhanced when compared to its in-plane bending modes, and vice versa when it is adsorbed perpendicular to the surface.[75,76] It is further seen that the vibrations involving atoms that are close to the silver surface will be more enhanced. When the wavenumber difference between the Raman bands in the normal and the SERS spectrum is not more than 5 cm^{-1}, the molecular plane will be perpendicular to the surface.[77] In 2-methylpyridine, Bunding *et al*.[78] noticed a significant shift and broadening of the CH_3 modes in the SERS spectrum. They explained this in terms of the interaction of the methyl group and the metal surface. In the present study, the symmetric methyl stretching mode is present in the SERS spectrum at 2933 cm^{-1} and is absent in the normal Raman spectrum. It should be related to the closeness of the methyl group to the silver surface. This is justifiable because the motion in groups directly interacting with the metal surface will be prominent in the SERS spectrum.[79] Further, the CH_2 and CH_3 bands at 1452, 1378, and 1149 cm^{-1} are also observed in the SERS spectrum, thereby supporting the above argument. In the case of SERS spectrum of β-hydroxy-β-methylbutanoic acid, the bands at 1447, 880, 725, and 692 cm^{-1} due to CH_2 and CH_3 modes suggest that these moieties assist the molecule to bind to the silver surface.[80] In the SERS spectrum of 2-amino-5-nitropyridine,[81] the symmetric NO_2 stretching mode corresponds to the most intense band, which appears broad and significantly downshifted from 1344 to 1326 cm^{-1} suggesting binding to silver through the lone pairs of the oxygen atom. Carrasco *et al*.[82] observed the NO_2 stretch in the SERS spectrum at ~1500 cm^{-1} with medium intensity, which demonstrated the importance of the nitro group in regard to the interaction with the metal surface. Further, they observed the enhancement of υPh modes, revealing that the molecule is oriented perpendicular to the metal surface, whereas the changes that occur in the nitro group indicate that the interaction occurs through oxygen atoms of the nitro moiety. The interaction induces a π-electronic redistribution primarily around both the nitro group and the aromatic portion in the vicinity of the substitution site. Also, Gao and Weaver[83] observed broadly and a downshift of the corresponding band of nitrobenzene adsorbed on gold via a nitro group. For the title compound, the symmetric stretching mode of NO_2 which is absent in the normal Raman spectrum appears at 1340 cm^{-1} in the SERS spectrum. Interaction through NO_2 group was also supported by the presence of modes at 1533, 730, and 534 cm^{-1}. For sodium salicylate,[74] the $\upsilon(C-O)_h$ stretch of the hydroxyl group is present in the SERS spectrum at 1252 cm^{-1} and this is indicative of the nearness of the OH group to the metal surface. In the present case, $\upsilon(C-O)_h$ appears at 1272 cm^{-1} with very strong intensity in the SERS spectrum.

Keeping in mind the behavior observed for molecules containing π-system adsorbed flat on the metal surfaces,[76,83–85] a purely parallel orientation of the molecular skeleton with respect to the surface appears unlikely in the light of the following arguments. The ring-breathing mode in the SERS spectrum at 829 cm^{-1} appears as a very weak band. Also, the out-of-plane CH modes 975,

914, and 906 cm^{-1} and the in-plane CH mode at 1072 cm^{-1} also suggest a tilted orientation of the molecule. The υPh modes are also present in the SERS spectrum at 1504, 1452, and 1430 cm^{-1}. In the SERS spectrum of the title compound, the aromatic CH stretching vibrations are observed as weak bands at 3050 and 3040 cm^{-1}, which suggests that the phenyl ring II may be in a position close to the perpendicular to the silver surface, possibly a tilted position since the bands are weak.[77,86,87]

Geometrical parameters and hyperpolarizability

To the best of our knowledge, no X-ray crystallographic data of this molecule has yet been established. However, the theoretical results obtained are almost comparable with the reported structure parameters of related molecules.[88–90] The carbon–oxygen (phenolate) $C_{12}-O_{31}$ distance of 1.3508 ´Å is in agreement with the average distance of 1.362 ´Å found among phenols.[91] DFT calculations give shortening of the angle $C_{17}-C_{15}-N_{33}$ by 0.6° and $C_{13}-C_{15}-N_{33}$ by 1° from 120° at C_{15} position and $C_{15}-N_{33}-O_{34}$, $C_{15}-N_{33}-O_{35}$ by 2.2° from 120° at N_{33} position. This reduction in angles reveals the hydrogen bonding between H_{19} and H_{16} atoms, which is evident from the increase in the angles $C_{17}-C_{15}-C_{13}$ by 1.5° and $O_{34}-N_{33}-O_{35}$ by 4.4°. The bond angles of the NO_2 group of the title compound $O_{34}-N_{33}-O_{35} = 124.4$, $O_{34}-N_{33}-C_{15} = 117.8$, and $O_{35}-N_{33}-C_{15} = 117.8$ are in agreement with the values 123.5, 118.7, and 117.9 given by Saeed *et al*.[90]

At C_3 position, the angle $C_4-C_3-C_{20}$ is reduced by 2.5° and $C_2-C_3-C_{20}$ is increased by 3.7° from 120°, and this asymmetry of exocyclic angles reveals the interaction between O_{24} and the phenyl ring II. The CC bond lengths in the phenyl ring lie between 1.3888 and 1.4153 ´Å, whereas for the phenyl ring II, the range is 1.3906–1.4032 ´Å. The CH bond lengths lie between 1.0826 and 1.0877 ´Å for phenyl ring I and between 1.0852 and 1.0876 ´Å for phenyl ring II. Here for the title compound, benzene is a regular hexagon with bond lengths somewhere in between the normal values for a singe (1.54 ´Å) and a double (1.33 ´Å) bond.[92] According to Noveron *et al*.,[88] for complexes of *N*-(4-pyridyl)benzamide, the bond lengths for $C_{11}-N_{25}$, $C_{20}-O_{24}$, $C_{20}-N_{25}$, $C_{20}-C_3$, C_3-C_2, C_3-C_4, and $N_{25}-H_{26}$ are 1.3953, 1.2253, 1.3703, 1.4943, 1.3923, 1.3933, and 0.773 ´Å, respectively, and the corresponding values for the title compound are 1.4128, 1.2210, 1.3933, 1.4977, 1.4019, 1.4016, and 1.0111 ´Å, respectively. For *N*-(2-pyridyl)benzamide complexes,[89] the bond lengths for $C_{20}-O_{24}$, $N_{25}-C_{20}$, $N_{25}-C_{11}$, and C_{20}-C_3 are 1.2445, 1.3646, 1.4156, and 1.4816 ´Å, respectively, while in the present case these bond lengths are 1.221, 1.3933, 1.4128, and 1.4977 ´Å.

The C═O and C–N bond lengths[23] in benzamide, acetamide, and formamide are, respectively, 1.2253, 1.2203, 1.2123 and 1.3801, 1.3804, 1.3683 ´Å.

According to the literature,[26,28,32,93] the changes in bond length in C═O and C–N are consistent with the following interpretation: that is, hydrogen bond decreases the double bond character of C═O bond and increases the double bond character of the C–N bond. The values of the angles $C_4-C_3-C_{20}$ (117.5°) and $C_3-C_{20}-O_{24}$ (122.7°) are smaller than those of benzaldehyde,[94] 121.0 and 123.6. These differences are ascribed to the steric repulsion between the H_8 and H_{26} atoms. The dihedral angle $C_2-C_3-C_{20}-O_{24}$ was determined to be −158.2° by the B3LYP method. On the contrary, the equilibrium structure of benzaldehyde is planar.[94] The steric repulsion in the present case is also considered to cause the nonplanar skeleton. The C_3-C_{20} bond length (1.4977 ´Å) is larger than the corresponding length of benzaldehyde[94] (1.4794 ´Å) by 0.0183 ´Å.

Saeed *et al*.[90] reported $C_{20}-O_{24}$, $N_{33}-O_{34}$, $N_{33}-O_{35}$, $N_{25}-C_{20}$, $N_{25}-C_{11}$, and N_{33}-C_{15} bond lengths are 1.2132, 1.2292, 1.2252, 1.3612, 1.4042, and 1.4632 ´Å for 2-nitro-*N*-(4-nitrophenyl)benzamide. For the title compound, the bond lengths obtained are 1.221, 1.2326, 1.2331, 1.3933, 1.4128, and 1.4614 ´Å, respectively. For the benzamide moiety of the title compound, the calculated values of the bond angles $C_{20}-N_{25}-C_{11}$, $C_{12}-C_{11}-N_{25}$, $O_{24}-C_{20}-N_{25}$, $O_{24}-C_{20}-C_3$, $N_{25}-C_{20}-C_3$, $C_4-C_3-C_{20}$, and $C_2-C_3-C_{20}$ are 122.7, 120.3, 122.1, 122.7, 115.2, 117.5, and 123.7°, respectively. Sun *et al*.[89] reported the corresponding angles as 124.7, 116.6, 123.1, 118.7, 118.3, 115.6, and 124.3°, respectively. Also, the DFT calculations give the torsional angles $C_{15}-C_{13}-C_{11}-N_{25}$, $N_{25}-C_{11}-C_{12}-C_{14}$, $O_{24}-C_{20}-C_3-C_2$, $N_{25}-C_{20}-C_3-C_2$, $O_{24}-C_{20}-C_3-C_4$, and $N_{25}-C_{20}-C_3-C_4$ as −178.3, −179.8, −158.2, 22.1, 20.8, and −158.9° around the benzamide group, which are in agreement with the reported values[88] 178.5, −178.9, −16.8, 163.8, 161.6, and −17.8°. The $C_{20}-N_{25}$ bond is twisted from the phenyl ring I and II, as is evident from the torsion angles $C_{12}-C_{11}-N_{25}-C_{20} = 60.5°$, $C_{13}-C_{11}-N_{25}-C_{20} = -122.0°$, and $N_{25}-C_{20}$-$C_3-C_4 = -158.9°$, $N_{25}-C_{20}-C_3-C_2 = 22.1°$.

Analysis of organic molecules having conjugated π-electron system×s and large hyperpolarizability using infrared and Raman spectroscopies has evolved as a subject of research.[95] The potential applications of the title compound in the field of nonlinear optics demand the investigation of its structural and bonding features contributing to the hyperpolarizability enhancement, by analyzing the vibrational modes using the IR and Raman spectra. The first hyperpolarizability (β_0) of this novel molecular system is calculated theoretically, based on the finite-field approach. In the presence of an applied electric field, the energy of a system is a function of the electric field. First hyperpolarizability is a third-rank tensor that can be described by a 3 3 × 3 matrix. The 27 components of the 3D matrix can be reduced to 10 components because of Kleinman symmetry.[96]

The components of β are defined as the coefficients in the Taylor-series expansion of the energy in the external electric field. When the electric field is weak and homogeneous, this expansion becomes

$$E = E_0 - \sum_i \mu_i F^i - \frac{1}{2}\sum_{ij} \alpha_{ij} F^i F^j - \frac{1}{6}\sum_{ijk} \beta_{ijk} F^i F^j F^k - \frac{1}{24}\sum_{ijkl} \gamma_{ijkl} F^i F^j F^k F^l + \ldots$$

where E_0 is the energy of the unperturbed molecule, F^i is the field at the origin, μ_i, α_{ij}, β_{ijk}, and γ_{ijkl} are the components of dipole moment, polarizability, the first hyper polarizabilities, and second hyperpolarizibilites, respectively. The calculated first hyperpolarizability of the title compound is 4.559×10^{-30} esu, which is comparable with the reported values of similar derivatives,[97] but the experimental value is not readily available. We conclude that the title compound is an attractive object for future studies of nonlinear optical properties.

In order to investigate the performance and vibrational wavenumbers of the title compound, the root mean-square (RMS) value and the correlation coefficient between calculated and observed wavenumbers were calculated (Fig. 5). RMS values of wavenumbers were evaluated using the following expression:[98]

$$RMS = \sqrt{\frac{1}{n-1}\sum_i^n (\upsilon_i^{calc} - \upsilon_i^{exp})^2}$$

Journal of RAMAN SPECTROSCOPY

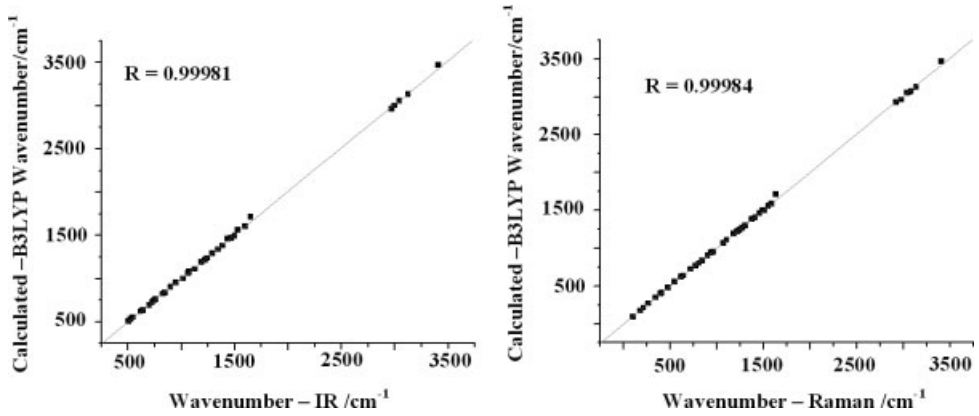

Figure 5. Correlation graph.

The RMS error of the observed Raman bands, IR bands, and the scaled wavenumbers are found to be 38.54, 36.86 (HF); 23.28, 23.8 (B3PW91); and 18.23, 18.11 (B3LYP), respectively. Small differences between experimental and calculated vibrational modes are observed. It must be due to the fact that hydrogen-bond vibrations present in the crystal lead to strong perturbation of the infrared wavenumbers and intensities of many other modes. Also, we state that the experimental results are of the solid phase and theoretical calculations are of the gaseous phase.

Conclusion

The FT-IR, FT-Raman, and SERS spectra of 4-ethyl-*N*-(2′-hydroxy-5′-nitrophenyl)benzamide were studied. The molecular geometry and the wavenumbers were calculated using different levels of theory. The observed wavenumbers are found to be in agreement with the calculated (B3LYP) values. The red shift of the NH stretching wavenumber in the IR spectrum from the computed wavenumber indicates the weakening of the NH bond resulting in proton transfer to the neighboring oxygen atom. The simultaneous IR and Raman activation of the C═O stretching modes gives the charge transfer interaction through a π-conjugated path. Optimized geometrical parameters of the title compound are in agreement with the reported values. SERS studies reveal a tilted orientation for the molecule and, the presence of methyl modes in the SERS spectrum indicates the nearness of methyl group to the metal surface.

Supporting information

Supporting information may be found in the online version of this article.

References

[1] A. Dalhoff, *Infection* **1994**, *22*, 111.
[2] V. Lee, S. Hecker, *J. Med. Chem.* **1999**, *19*, 521.
[3] D. Livermore, *Int. J. Antimicrob. Agents* **2000**, *16*, 3.
[4] K. Poole, *Curr. Opin. Microbiol. Agents* **2001**, *4*, 500.
[5] D. Abbant, M. Macielag, K. Bush, *Expert Opin. Investig. Drugs* **2003**, *12*, 379.
[6] H. Mrozik, H. Jones, J. Friedman, G. Schwartzkopf, R. Schardt, A. Patchett, D. R. Holff, J. J. Yakstis, R. F. Riek, D. A. Ostlind, G. A. Plischker, R. W. Butler, A. C. Cuckler, W. C. Campbell, *Experientia* **1969**, *25*, 883.
[7] S. Itaru, M. Seizo, K. Takashi, *Chem. Abstr.* **1973**, *81*(1974), 73387, Japan Patent, 73, 37, 819.
[8] P. I. Braz Pedido, *Chem. Abstr.* **1981**, *95*(1981), 61812z, N80 04, 641.
[9] G. A. White, *Pestic. Biochem. Physiol.* **1989**, *34*, 255.
[10] I. Yalcin, B. K. Kaymakcioglu, I. Oren, E. Sener, O. Temiz, A. Akin, N. Altanlar, *Il Farmaco* **1997**, *52*, 685.
[11] K. J. Pradhan, P. S. Variyar, J. R. Bandekar, *Lebensm. Wiss. U-Technol.* **1999**, *32*, 121.
[12] E. Aki-Sener, K. K. Bingol, I. Oren, O. Temiz-Arpaci, I. Yalcin, I. N. Altanlar, *Il Farmaco* **2000**, *55*, 469.
[13] E. Aki-Sener, K. K. Bingol, O. Temiz-Arpaci, I. Yalcin, N. Altnlar, *Il Farmaco* **2002**, *57*, 451.
[14] I. Yildiz-Oren, E. Aki-Sener, C. Ertas, O. Temiz-Arpaci, I. Yalcin, N. Altanlar, *Turk. J. Chem.* **2004**, *28*, 441.
[15] I. Kobayashi, H. Muraoka, M. Hasegawa, T. Saika, M. Nishida, M. Kawamura, R. Ando, *J. Antimicrob. Chemother.* **2002**, *50*, 129.
[16] T. Ertan, I. Yildiz, S. Ozkan, O. Temiz-Arpaci, F. Kaynak, I. Yalcin, E. Aki-Sener, U. Abbasoglu, *Bioorg. Med. Chem.* **2007**, *15*, 2032.
[17] J. Vinsova, A. Imramovsky, *Cesk. Slov. Farm.* **2004**, *53*, 294.
[18] R. De La Fluente, N. D. Sonawane, D. Arumainayagam, A. S. Verkaman, *Br. J. Pharmacol.* **2006**, *149*, 551.
[19] J. Vinsova, A. Imramovsky, V. Buchta, M. Ceckova, M. Dolezal, F. Staud, J. Jampilek, J. Kaustova, *Molecules* **2007**, *11*, 1.
[20] M. K. Dahlgren, A. M. Kauppi, I. M. Olsson, A. Linusson, M. Elofsson, *J. Med. Chem.* **2007**, *50*, 6177.
[21] K. Waisser, J. Matyk, H. Divisova, P. Husakova, J. Kunes, V. Klimesova, J. Kaustova, U. Moellmann, H. M. Cause, M. Miko, *Arch. Pharm.* **2006**, *149*, 616.
[22] H. Arslan, U. Florke, N. Kulcu, G. Binzet, *Spectrochim. Acta* **2007**, *68A*, 1347.
[23] H. Takeuchi, M. Sato, T. Tsuji, H. Takashima, T. Egawa, S. Konaka, *J. Mol. Struct.* **1999**, *485-486*, 175.
[24] M. Kitano, K. Kuchitsu, *Bull. Chem. Soc. Jpn.* **1974**, *47*, 67.
[25] M. Kitano, K. Kuchitsu, *Bull. Chem. Soc. Jpn.* **1973**, *46*, 3048.
[26] E. D. Stevens, *Acta Crystallogr.* **1978**, *B34*, 544.
[27] J. Ladell, B. Post, *Acta Crystallogr.* **1954**, *7*, 559.
[28] T. Otterson, *Acta Chem. Scand.* **1975**, *A29*, 939.
[29] G. A. Jeffrey, J. R. Ruble, R. K. McMullan, D. J. DeFrees, J. S. Binkley, J. A. Pople, *Acta Crystallogr.* **1980**, *B36*, 2292.
[30] W. A. Denne, R. W. H. Small, *Acta Crystallogr.* **1971**, *B27*, 1094.
[31] C. C. F. Blake, R. W. H. Small, *Acta Crystallogr.* **1972**, *B28*, 2201.
[32] Q. Gao, G. A. Jeffrey, J. R. Ruble, R. K. McMullan, *Acta Crystallogr.* **1991**, *B47*, 742.
[33] Y. S. Choi, J. Kim, J. Park, J. A. Yu, C. J. Yoon, *Spectrochim. Acta* **1996**, *52A*, 1779.
[34] P. Kawski, A. Kochel, M. G. Perevozkina, A. Filarowski, *J. Mol. Struct.* **2006**, *790*, 65.
[35] N. C. Handy, C. W. Murray, R. D. Amos, *J. Phys. Chem.* **1993**, *97*, 4392.
[36] P. J. Stephens, F. J. Delvin, C. F. Chavalowski, M. J. Frisch, *J. Phys. Chem.* **1994**, *98*, 11623.
[37] F. J. Delvin, J. W. Finley, P. J. Stephens, M. J. Frisch, *J. Phys. Chem.* **1995**, *99*, 16883.
[38] S. Y. Lee, B. H. Boo, *Bull. Korean chem. Soc.* **1996**, *17*, 754.
[39] S. Y. Lee, B. H. Hoo, *Bull. Korean Chem. Soc.* **1996**, *17*, 760.

[40] G. Rauhut, P. Pulay, *J. Phys. Chem.* **1995**, *99*, 3093.
[41] A. D. Becke, *J. Chem. Phys.* **1993**, *98*, 5648.
[42] P. C. Lee, D. J. Meisel, *J. Phys. Chem.* **1982**, *86*, 3391.
[43] M. J. Frisch, G. W. Trucks, H. B. Schlegel, G. E. Scuseria, M. A. Robb, J. R. Cheeseman, J. A. Montgomery, Jr., T. Vreven, K. N. Kudin, J. C. Burant, J. M. Millam, S. S. Iyengar, J. Tomasi, V. Barone, B. Mennucci, M. Cossi, G. Scalmani, N. Rega, G. A. Petersson, H. Nakatsuji, M. Hada, M. Ehara, K. Toyota, R. Fukuda, J. Hasegawa, M. Ishida, T. Nakajima, Y. Honda, O. Kitao, H. Nakai, M. Klene, X. Li, J. E. Knox, H. P. Hratchian, J. B. Cross, C. Adamo, J. Jaramillo, R. Gomperts, R. E. Stratmann, O. Yazyev, A. J. Austin, R. Cammi, C. Pomelli, J. W. Ochterski, P. Y. Ayala, K. Morokuma, G. A. Voth, P. Salvador, J. J. Dannenberg, V. G. Zakrzewski, S. Dapprich, A. D. Daniels, M. C. Strain, O. Farkas, D. K. Malick, A. D. Rabuck, K. Raghavachari, J. B. Foresman, J. V. Ortiz, Q. Cui, A. G. Baboul, S. Clifford, J. Cioslowski, B. B. Stefanov, G. Liu, A. Liashenko, P. Piskorz, I. Komaromi, R. L. Martin, D. J. Fox, T. Keith, M. A. Al-Laham, C. Y. Peng, A. Nanayakkara, M. Challacombe, P. M. W. Gill, B. Johnson, W. Chen, M. W. Wong, C. Gonzalez, J. A. Pople, *Gaussian 03, Revision C. 02*, Gaussian: Wallingford, **2004**.
[44] J. B. Foresman, in *Exploring Chemistry with Electronic Structure Methods: A Guide to Using Gaussian* (Ed.: E. Frisch), Gaussian: Pittsburg, PA, **1996**.
[45] A. P. Scott, L. Radom, *J. Phys. Chem.* **1996**, *100*, 16503.
[46] P. Flukiger, H. P. Luthi, S. Portmann, J. Weber, *MOLEKEL, 4.3*, Swiss Center for Scientific Computing: Manno, Switzerland, **2000**.
[47] S. Portmann, H. P. Luthi, *Chimia* **2000**, *54*, 766.
[48] N. P. G. Roeges, *A Guide to the Complete Interpretation of Infrared Spectra of Organic Structures*, Wiley: New York, **1994**.
[49] G. Varsanyi, *Assignments of Vibrational Spectra of Seven Hundred Benzene Derivatives*, Wiley: New York, **1974**.
[50] N. B. Colthup, L. H. Daly, S. E. Wiberly, *Inroduction to Infrared and Raman spectroscopy* (3rd edn), Academic Press: Boston, **1990**.
[51] G. Varsanyi, P. Sohar, *Acta Chim. Acad. Sci. Hung.* **1973**, *76*, 243.
[52] A. S. El-Shahawy, S. M. Ahmed, N. K. Sayed, *Spectrochim. Acta* **2007**, *66*, 143.
[53] R. M. Silverstein, G. C. Bassler, T. C. Morril, *Spectrometric Identification of Organic Compounds* (5th edn), John Wiley and Sons Inc: Singapore, **1991**.
[54] M. Barthes, G. De Nunzio, G. Riber, *Synth. Met.* **1996**, *76*, 337.
[55] C. Y. Panicker, H. T. Varghese, D. Philip, H. I. S. Nogueira, K. Kastkova, *Spectrochim. Acta* **2007**, *67*, 1313.
[56] A. Perjessy, D. Rasala, P. Tomasik, R. Gawinecki, *Collect. Czech. Chem. Commun.* **1985**, *50*, 244.
[57] J. F. Brown Jr, *J. Am. Chem. Soc.* **1955**, *77*, 6341.
[58] J. H. S. Green, W. Kynanston, A. S. Lindsery, *Spectrochim. Acta* **1961**, *17*, 486.
[59] O. Exner, S. Kovac, E. Solcaniova, *Collect. Czech. Chem. Commun.* **1972**, *37*, 2156.
[60] D. S. Ranga Rao, G. Thyagarajan, *Indian J. Pure Appl. Phys.* **978**, *16*, 941.
[61] N. Sundaraganesan, S. Ayyappan, H. Umamaheswari, B. D. Joshua, *Spectrochim. Acta* **2007**, *66A*, 17.
[62] R. Shanmugam, D. Sathyanarayana, *Spectrochim. Acta* **1984**, *40A*, 764.
[63] A. Bigotto, B. Pergolese, *J. Raman Spectrosc.* **2001**, *32*, 953.
[64] N. Sandhyarani, G. Skanth, S. Berchmanns, V. Yegnaraman, T. Pradeep, *J. Colloid Interface Sci.* **1999**, *209*, 154.
[65] P. L. Anto, C. Y. Panicker, H. T. Varghese, D. Philip, O. Temiz-Arpaci, B. T. Gulbas, I. Yildiz, *Spectrochim. Acta* **2007**, *67A*, 744.
[66] P. Sett, N. Paul, S. Chattopadhyay, P. K. Mallick, *J. Raman Spectrosc.* **1999**, *30*, 277.
[67] P. Sett, S. Chattopadhyay, P. K. Mallick, *Spectrochim. Acta* **2000**, *56A*, 855.
[68] P. Sett, S. Chattopadhyay, P. K. Mallick, *J. Raman Spectrosc.* **2000**, *31*, 177.
[69] V. Volvosek, G. Baranovic, L. Colombo, J. R. Durig, *J. Raman Spectrosc.* **1991**, *22*, 35.
[70] M. Muniz-Miranda, E. Castelluci, N. Neto, G. Sbrena, *Spectrochim. Acta* **1983**, *39A*, 107.
[71] J. H. S. Green, *Spectrochim. Acta* **1968**, *24*, 1627.
[72] Y. S. Mary, H. T. Varghese, C. Y. Panicker, T. Ertan, I. Yildiz, O. Temiz-Arpaci, *Spectrochim. Acta* **2008**, *71*, 566.
[73] A. R. Amjujakshan, V. S. Madhavan, H. T. Varghese, C. Y. Panicker, O. Temiz-Arpaci, B. Tekiner-Gulbas, I. Yildiz, *Spectrochim. Acta* **2007**, *69A*, 782.
[74] D. Philip, A. John, C. Y. Panicker, H. T. Varghese, *Spectrochim. Acta* **2001**, *57*, 1561.
[75] J. A. Creighton, *Spectroscopy of Surfaces, Advance in Spectroscopy*, vol. 16, Wiley: New York, **1988**, pp 37, Chapt. 2.
[76] X. Gao, J. P. Davies, M. J. Weaver, *J. Phys. Chem.* **1990**, *94*, 6858.
[77] G. Levi, J. Patigny, J. A. Massult, J. Aubard, *ICORS, Proceedings of the 13th International Conference in Raman spectroscopy*, Wurzburg, **1992**, p 652.
[78] K. A. Bunding, J. R. Lombardi, R. L. Birke, *Chem. Phys.* **1980**, *49*, 53.
[79] S. Kai, W. Chaozhi, X. Guangzhi, *Spectrohcim. Acta* **1989**, *45A*, 1029.
[80] E. Podstawka, M. Swiatlowska, E. Borowiec, L. M. Proniewicz, *J. Raman Spectrosc.* **2006**, *38*, 356.
[81] M. M. Maurizio, *Vib. Spectrosc.* **2002**, *29*, 229.
[82] E. A. Carrasco, F. M. Compos-Vallette, P. Leyton, G. Diaz, R. E. Clavijo, J. V. Garcia-Ramos, N. Inostroza, C. Domingo, S. Sanchez-Cortes, R. Koch, *J. Phys. Chem.* **2003**, *107*, 9611.
[83] P. Gao, M. J. Weaver, *J. Phys. Chem.* **1985**, *89*, 5040.
[84] M. L. Patterson, M. J. Weaver, *J. Phys. Chem.* **1985**, *89*, 5046.
[85] Y. J. Kwon, D. H. Son, S. J. Ahn, M. S. Kim, K. Kim, *J. Phys. Chem.* **1994**, *98*, 8481.
[86] J. A. Creighton, *Surf. Sci.* **1983**, *124*, 209.
[87] J. S. Suh, M. Moskovits, *J. Am. Chem. Soc.* **1986**, *108*, 4711.
[88] J. C. Noveron, A. M. Arif, P. J. Stang, *Chem. Mater.* **2003**, *15*, 372.
[89] W. H. Sun, W. Zhang, T. Gao, X. Tang, L. Chen, Y. Li, X. Jin, *J. Organomet. Chem.* **2004**, *689*, 917.
[90] A. Saeed, S. Hussain, U. Florke, *Turk. J. Chem.* **2008**, *32*, 1.
[91] F. H. Allen, O. Kennard, D. G. Watson, L. Brammer, A. G. Orpen, R. Taylor, *J. Chem. Soc. Perkin Trans.* **1987**, *2*, S1.
[92] P. Sykes, *A Guide Book to Mechanism in Organic Chemistry* (6th edn), Pearson Education: New Delhi, India, **2004**.
[93] J. L. Katz, B. Post, *Acta Crystallogr.* **1960**, *13*, 624.
[94] K. B. Borisenko, C. W. Bock, I. Hargittai, *J. Phys. Chem.* **1996**, *100*, 7426.
[95] M. Tommasini, C. Castiglioni, M. Del Zoppo, G. Zerbi, *J. Mol. Struct.* **1999**, *480*, 179.
[96] D. A. Kleinman, *Phys. Rev.* **1962**, *126*, 1977.
[97] H. T. Varghese, C. Y. Panicker, V. S. Madhavan, S. Mathew, J. Vinsova, C. Van Alsenoy, **2009**, *40*, 1211.
[98] L. Ushakumari, H. T. Varghese, C. Y. Panicker, T. Ertan, I. Yildiz, *J. Raman Spectrosc.* **2008**, *39*, 1832.